Available online www.jsaer.com

***Journal of Scientific and Engineering Research*, 2020, 7(9):25-34**

Research Article

ISSN: 2394-2630
CODEN(USA): JSERBR

Unsteady MHD boundary layer flow with Joule heating and viscous dissipation along a vertical permeable plate in presence of ion-slip current and high porosity medium

Md. Jamal Hossain, *Md. Delowar Hossain

Project Director, Establishment of Polytechnic Institute in 23 Districts, Directorate of technical education, Dhaka. Bangladesh
Department of Mathematics,, Chittagong University of Engineering & Technology, Chittagong, Bangladesh
*Corresponding author: delowar@cuet.ac.bd

Abstract In this paper unsteady combined effects of Joule heating and viscous dissipation on MHD free convection flow past a vertical permeable plate with high porosity medium in presence of ion-slip current has been studied numerically. The finite difference method is used to solve the non-dimension governing equations. The governing equations are transformed into dimensionless coupled nonlinear ordinary differential equations by using usual transformations. The numerical results of the velocities such as primary and secondary velocities and temperature profiles for different physical parameters entering into the problem are investigated. The velocity, rate of change of velocity, temperature profiles and rate of change of temperature are displayed in the form of graph.

Keywords MHD, Ion-slip effects, Viscous dissipation, Joule heating, Porosity

1. Introduction

The effect of free convection on the accelerated flow of a viscous incompressible fluid past an infinite vertical porous plate with suction has many important technological applications in the astrophysical, geophysical and engineering problems such as catalytic reactors and compact heat exchangers, in geothermal energy convection, fibrous materials in the thermal insulation of buildings, in the heat transfer from storage of agricultural products. It was shown by Gebhart [1] that the viscous dissipation effect plays an important role in natural convection in viscous devices that are subjected to large deceleration or which operate at high rotative speeds and also in strong gravitational field processes on large scales (on large planets) and geological process. Hall and ion-slip currents have important on the magnitude and direction of the current density and consequently on the magnetic force term. MHD natural convection flow with Hall and ion-slip currents has many important engineering applications, e.g. in power generators, Hall accelerators and flows in channels and ducts. At first Vafai and Tien [2] studied boundary and inertia effects on flow and heat transfer in a porous media of constant and variable porosity. They have observed that the great influence of the variation of porosity and permeability take place in velocity and heat transfer. Schwartz and Smith [3] investigated and reported porosity is not constant but varies from the wall to the interior due to variation in permeability. Magnetohydrodynamic non-Darcy free and force convection heat transfer from a vertical heated plate surrounded in a permeable medium with variable porosity investigated by Pal [4]. MHD natural onvection heat and mass transfer from a sphere in a variable porosity regime with thermal radiation have studied by Prasad et al [5]. Al-Humoud and Chamkha [6] analyzed double diffusive convection of a rotating fluid over a surface embedded in a thermally stratified high porosity medium. Poonia and Chaudhary [7] studied MHD free convection and mass transfer flow over an infinite vertical plate

with viscous dissipation. Foisal and Alam [8] analyzed unsteady free convection fluid flow over an inclined plate in the presence of a magnetic field with thermally stratified high porosity medium. Mahender and Rao [9] investigated unsteady MHD free convection and mass transfer flow past a porous plate in presence of viscous dissipation. Jaber [10] discussed the effects of viscous dissipation and Joule heating on MHD flow of a fluid with variable properties past a stretching vertical plate. Thermally stratified high porosity medium in a revolving fluid surrounded along a upright plate have examined Chamkha et al. [11]. Chen et al.[12] have analyzed transient free convection on a vertical flat plate surrounded in a high porosity medium. Bhuvanavijaya and Mallikarjuna [13] investigated the effect of variable thermal conductivity on convective heat and mass transfer over a vertical plate in a rotating system with variable porosity regime. Anjali Devi et al. [14] dicussed Hall effect on unsteady MHD free convection flow past an impulsively started porous plate with viscous and Joule's dissipation. Lakshmanna1 and Venkateswarlu [15] demonstrated unsteady MHD convective flow of an incompressible viscous fluid through porous medium over a vertical plate. Abdou [16] investigated the effects of MHD and Joule heating on free convective boundary layer with a variable plate temperature in a porous medium.

Hence our aim is to investigate the combined effects of Joule heating and viscous dissipation on MHD natural convection flow along a erect porous plate with high porosity media and ion-slip current have been considered. Finite difference method is used to solve the dimensionless nonlinear coupled partial differential equations. The velocities such as primary and secondary velocities, rate of change of velocity, temperature and rate of change of temperature are presented in graphical form.

2. Governing Equations

Unsteady boundary layer flow of an electrically conducting viscous incompressible fluid over an infinite upright permeable plate $y=0$ in presence of magnetic field have been considered. The flow is upward direction along the erect plate which is considered in x - axis. The y -axis is considered perpendicular to the flow direction. A strong magnetic field $\mathbf{B}$ is imposed along y -axis and the plate is taken electrically non-conducting. Since the plate is infinite in extent, all physical quantities are functions of y and t only. The magnetic Reynolds number of a partially-ionized fluid is very small, so the induced magnetic field is neglected. If $\mathbf{J}=\left(J_x, J_{y,} J_z\right)$ is the current density, from the relation $\overline{\nabla}\cdot\mathbf{J}=0$ gives $J_y=$ constant. Since the plate is electrically non-conducting, $J_y=0$ at the plate and hence zero everywhere. The configuration and coordinate system of the model are shown in Fig.1. Due to magnetic field the Hall and ion-slip currents are significantly affected in the flow. The governing equations of the flow under the above consideration and Boussinesq's approximation are as follows:

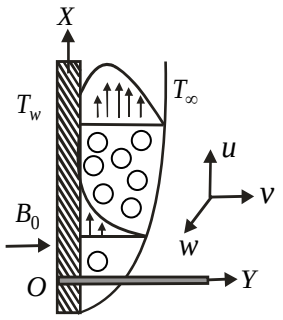

Figure 1: Physical configuration and coordinate system

Continuity equation; $$\frac{\partial v}{\partial y}=0 \tag{1}$$

Momentum equation;

$$\frac{1}{\varepsilon^2}\left(\frac{\partial u}{\partial t}+v\frac{\partial u}{\partial y}\right)=\frac{\upsilon}{\varepsilon}\frac{\partial^2 u}{\partial y^2}+g\beta\left(T-T_\infty\right)-\frac{\upsilon}{k}u-cu^2-\frac{\sigma_e B_0^2}{\rho\left(\alpha_e^2+\beta_e^2\right)}\left(\alpha_e u+\beta_e w\right) \tag{2}$$

$$\frac{1}{\varepsilon^2}\left(\frac{\partial w}{\partial t}+v\frac{\partial w}{\partial y}\right)=\frac{\upsilon}{\varepsilon}\frac{\partial^2 w}{\partial y^2}-\frac{\upsilon}{k}w-cw^2+\frac{\sigma_e B_0^2}{\rho\left(\alpha_e^2+\beta_e^2\right)}\left(\beta_e u-\alpha_e w\right) \tag{3}$$

Energy equation;

$$\frac{\partial T}{\partial t}+v\frac{\partial T}{\partial y}=\frac{\kappa}{\rho c_p}\frac{\partial^2 T}{\partial y^2}+\frac{\upsilon}{c_p}\left[\left(\frac{\partial u}{\partial y}\right)^2+\left(\frac{\partial w}{\partial y}\right)^2\right]+\frac{\sigma_e B_0^2}{\rho c_p\left(\alpha_e^2+\beta_e^2\right)}\left(u^2+w^2\right) \tag{4}$$

The boundary conditions for the model are as follows;

$$\left.\begin{array}{l} u(y,t)=U_0, w(y,t)=0, T(y,t)=T_w \quad at\ y=0 \\ u(y,t)=0, w(y,t)=0, T(y,t)=T_\infty \quad at\ y\to\infty \end{array}\right\} \tag{5}$$

where U_0 is the uniform velocity, $\alpha=1+\beta_e\beta_i$, β_e is the Hall current parameter, β_i is the ion-slip current parameter, y is Cartesian co-ordinate, u and w are the components of flow velocity, g is the acceleration due to gravity, β is the coefficient of volumetric thermal expansion of the fluid, ρ is the density, υ is the viscosity, k is the magnetic permeability, σ_e is the electrical conductivity of the fluid, κ is the thermal conductivity, c_p is the specific heat at constant pressure, c is the Forcheimmer (inertial) coefficient, ε is the porosity of porous medium,

Now a convenient solution of equation (1) is $v=-v_0$ (constant) (6)

where the constant v_0 represents the normal velocity at the plate which is positive or negative for suction or blowing. Using equation (6), the equations (2)-(4) become

Momentum Equation:

$$\frac{1}{\varepsilon^2}\left(\frac{\partial u}{\partial t}-v_0\frac{\partial u}{\partial y}\right)=\frac{\upsilon}{\varepsilon}\frac{\partial^2 u}{\partial y^2}+g\beta(T-T_\infty)-\frac{\upsilon}{k}u-cu^2-\frac{\sigma_e B_0^2}{\rho\left(\alpha_e^2+\beta_e^2\right)}\left(\alpha_e u+\beta_e w\right) \tag{7}$$

$$\frac{1}{\varepsilon^2}\left(\frac{\partial w}{\partial t}-v_0\frac{\partial w}{\partial y}\right)=\frac{\upsilon}{\varepsilon}\frac{\partial^2 w}{\partial y^2}-\frac{\upsilon}{k}w-cw^2+\frac{\sigma_e B_0^2}{\rho\left(\alpha_e^2+\beta_e^2\right)}\left(\beta_e u-\alpha_e w\right) \tag{8}$$

Energy equation:

$$\frac{\partial T}{\partial t}-v_0\frac{\partial T}{\partial y}=\frac{\kappa}{\rho c_p}\frac{\partial^2 T}{\partial y^2}+\frac{\upsilon}{c_p}\left[\left(\frac{\partial u}{\partial y}\right)^2+\left(\frac{\partial w}{\partial y}\right)^2\right]+\frac{\sigma_e B_0^2}{\rho c_p}\left(u^2+w^2\right) \tag{9}$$

The boundary conditions for the model are as follows;

$$\left.\begin{array}{l} u(y,t)=U_0, w(y,t)=0, T(y,t)=T_w \quad at\ y=0 \\ u(y,t)=0, w(y,t)=0, T(y,t)=T_\infty \quad at\ y\to\infty \end{array}\right\} \tag{10}$$

For the purpose of solving the system of equation numerically, the transformation of governing equations into non-dimensional variables is introduced as follows;

$$Y=\frac{yU_0}{\upsilon}, U=\frac{u}{U_0}, W=\frac{w}{U_0}, \tau=\frac{tU_0^2}{\upsilon}, \bar{T}=\frac{T-T_\infty}{T_w-T_\infty} \tag{11}$$

Thus introducing the relation (11) in equations (7)-(9), the following dimensionless differential equations have been obtained as follows;

$$\frac{\partial U}{\partial \tau}-\lambda\frac{\partial U}{\partial Y}=\varepsilon\frac{\partial^2 U}{\partial Y^2}+\varepsilon^2 G_r\bar{T}-\varepsilon^2\gamma U-\varepsilon^2\Gamma\left(U^2+W^2\right)-\frac{M\varepsilon^2\left(\alpha_e U+\beta_e W\right)}{\alpha_e^2+\beta_e^2} \tag{12}$$

$$\frac{\partial W}{\partial \tau}-\lambda\frac{\partial W}{\partial Y}=\varepsilon\frac{\partial^2 W}{\partial Y^2}-\varepsilon^2\gamma W-\varepsilon^2\Gamma\left(U^2+W^2\right)+\frac{M\varepsilon^2\left(\beta_e U-\alpha_e W\right)}{\alpha_e^2+\beta_e^2} \tag{13}$$

$$\frac{\partial T}{\partial \tau}-\lambda\frac{\partial T}{\partial Y}=\frac{1}{p_r}\frac{\partial^2 \bar{T}}{\partial Y^2}+E_c\left[\left(\frac{\partial U}{\partial Y}\right)^2+\left(\frac{\partial W}{\partial Y}\right)^2\right]+\frac{ME_c\left(U^2+W^2\right)}{\alpha_e^2+\beta_e^2} \tag{14}$$

where $\lambda=\frac{v_0}{U_0}$ is the suction parameter, $G_r=\frac{g_0\beta\left(T_w-T_\infty\right)\upsilon}{U_0^2}$ is the Grashof number, $M=\frac{\sigma_e B_0^2\upsilon}{\rho U_0^2}$ is the magnetic parameter, $P_r=\frac{\rho\upsilon c_p}{\kappa}$ is the Prandtl number, $\gamma=\frac{\upsilon^2}{kU_0^2}$ is the permeability parameter, $\Gamma=\frac{c\upsilon}{U_0}$ is the inertial parameter, $E_c=\frac{U_0^2}{c_p\left(T_w-T_\infty\right)}$ is the Eckert number.

The corresponding boundary conditions are as follows;

$$\left.\begin{array}{l} U(y,\tau)=1, W(y,\pi t)=0, \bar{T}(y,\tau)=1 \quad at\ Y=0 \\ U(y,\tau)=0, W(y,\tau)=0, \bar{T}(y,\tau)=0 \quad at\ Y\to\infty \end{array}\right\} \tag{15}$$

3. Solution Technique

The finite difference method is used to solve the dimensionless non-linear coupled partial differential equations (12)-(14) with boundary conditions (15). The region within the boundary layer is divided by some perpendicular lines of Y -axis, where Y -axis is normal to the medium is shown Fig.2. The maximum length of boundary layer is assumed $Y_{\max}(=50)$ as corresponds to $Y\to\infty$ i.e. Y varies from 0 to 50 and number of grid spacing in Y -direction is $m(=400)$, hence the constant mesh size along Y -axis becomes $\Delta Y=0.13(0\le Y\le 50)$ with a smaller time step $\Delta\tau=0.001$.

4. Shear stress and Nusselt number

The rate of change of velocity (shear stress), temperature (Nusselt number) at the plate of the model is investigated. Those are presented in graphical form. The following equations represent the rate of change of velocity in x and z axes are as follows;

$\tau_U=\mu\left(\frac{\partial u}{\partial y}\right)_{y=0}$ and $\tau_W=\mu\left(\frac{\partial w}{\partial y}\right)_{y=0}$ which are proportional to $\left(\frac{\partial U}{\partial Y}\right)_{Y=0}$ and $\left(\frac{\partial W}{\partial Y}\right)_{Y=0}$.

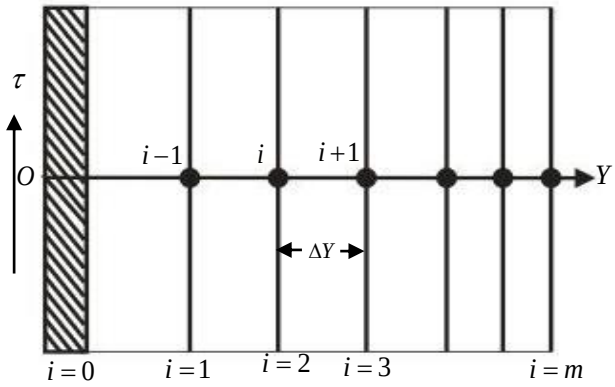

Figure 2: Finite difference grid space

From the temperature field, the effects of various parameters on the heat transfer coefficients have been studied. The following relations represent the heat transfer rate that is well known Nusselt number. Nusselt number is $N_u=-k\left(\frac{\partial T}{\partial y}\right)_{y=0}$ which is proportional to $\left(\frac{\partial \bar{T}}{\partial Y}\right)_{Y=0}$.

The numerical values of the shear stress and Nusselt number are calculated by five point approximate formula for the derivatives.

5. Results and Discussion

The numerical solution was obtained for distributions of the dimensionless primary velocity (U), secondary velocity (W), temperature ($\bar{T}$) as well as the shear stress in x -axis (τ_U), shear stress in z -axis (τ_W) and Nusselt number (N_u). The effects of velocity, rate of change of velocity, temperature and rate of change of temperature profiles are drawn for various values of the parameters that describe in the flow, e.g. Hall parameter (β_e), ion-slip parameter (β_i), magnetic parameter (M), suction parameter (λ), permeability parameter (γ), Eckert number (E_c), porosity(ε), inertial parameter (Γ), Pramdtl number (P_r), Grashof number(G_r). The values of Prandtl number are chosen $P_r=0.71$ (Prandtl number for air at 20^0C), to $P_r=1.0$ (Prandtl number for salt water at 20^0C), $P_r=1.63$ (corresponds glycerin at 50^0C), which represent the specific condition of the flow. The values of G_r is taken to be large ($G_r=5.0$).

From Figures 3 (a,b) illustrated that , primary velocity (U) and shear stress in x -axis (τ_U) are increased with the increase of ion-slip parameter β_i. The effective conductivity decreases with the increase of β_i which reduces the magnetic damping force on primary velocity. It is found that secondary velocity and shear stress in

z -axis (τ_W) profiles have reverse effect for increasing values ion-slip parameter which are displayed in Figures. 4(a,b).

The primary velocity (U), rate of change of velocity in x-axis (τ_U) profiles are increased with the increasing values of Eckert number (E_c) which are displayed in Figures. 5(a,b).This is due to the heat energy stored in the liquid because of the frictional heating. The temperature distributions in flow region are enhanced with the increasing values of Eckert number (E_c) which is found in Figure. 6(a). The viscous dissipation will lead to a heat generation inside the fluid. For this reason heat energy is stored in the fluid due to the frictional heating. But Nusselt number (N_u) has reverse effect which is shown in Figure. 6(b).

Figures 7(a,b) illustrate that the primary velocity (U), shear stress in x -axis (τ_U) increase with increasing values of porosity (ε). Increasing porosity clearly serves to enhance the flow velocity i.e. accelerates the flow. Whereas secondary velocity W , shear stress in z -axis (τ_W) profiles have reverse effect which are found in Figures. 8(a,b).

From Figures. 9(a,b), it has been seen that the primary velocity U and shear stress in x -axis (τ_U) decreases with an increase in magnetic parameter M . This is due to the fact that, the transverse magnetic field normal to the flow direction, has a tendency to create the drag force which is known as the Lorentz force which tends to resist the flow .

In Figures 10(a,b) illustrated that the primary velocity (U) and shear stress in x -axis (τ_U) profiles decrease with the increase of Prandtl number(P_r). This is because in the free convection the plate velocity is higher than the adjacent fluid velocity and the momentum boundary layer thickness decreases. Figure 11(a) illustrated that the temperature distributions are decreased with the increase of Prandtl number. Because the thermal diffusivity decreases and these phenomena lead to the decreasing of energy ability that reduces the thermal boundary layer. Nusselt number (N_u) increases with the increase of Prandtl number which is found in Figue 11(b). The increase of Prandtl number means slow rate of thermal-diffusion.

Figures 12 (a,b) displayed that the primary velocity (U) and rate of change of velocity in x -axis (τ_U) are decreased with the increase of permeability parameter (γ). Because permeable parameter has tendency to slow down the flow motion.

Figures 13 (a,b) are displayed that the primary velocity (U) and rate of change of velocity in x -axis (τ_U) are decreased with the increase of suction parameter (λ). Because the suction parameter stabilized the boundary layer growth.

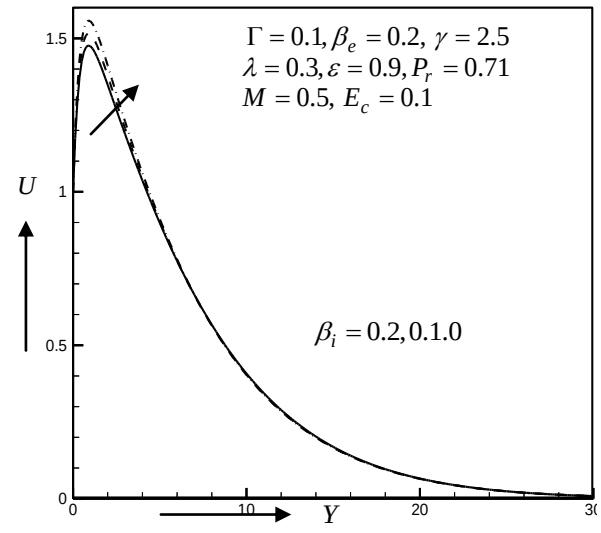

Figure 3(a): Primary velocity profiles for different values of ion-slip parameter

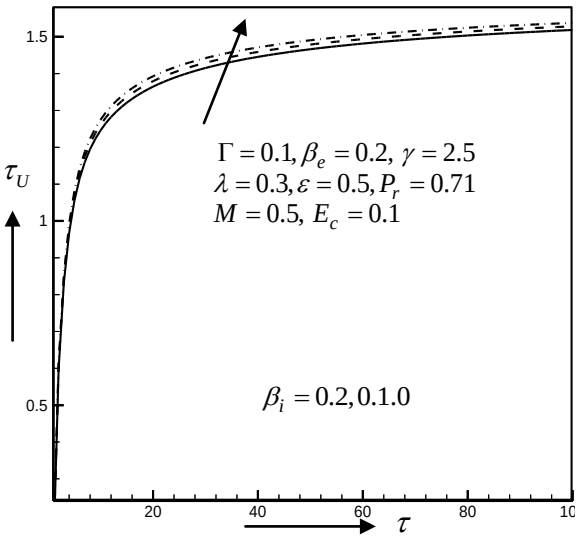

Figure 3(b): Shear stress in x -axis for different values of ion-slip parameter

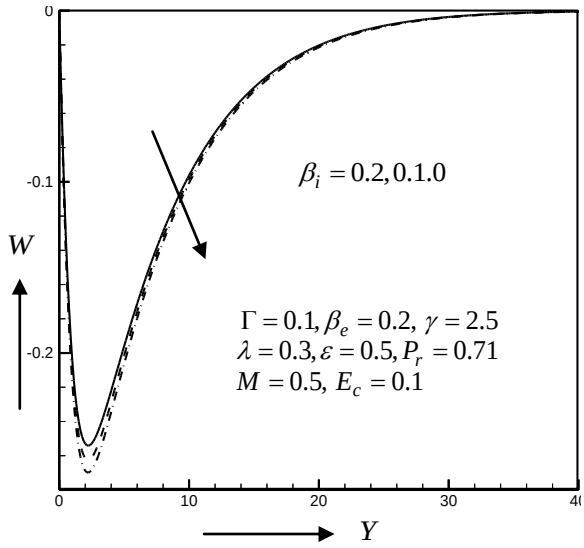

Figure 4(a): secondary velocity profiles for different values of ion-slip parameter

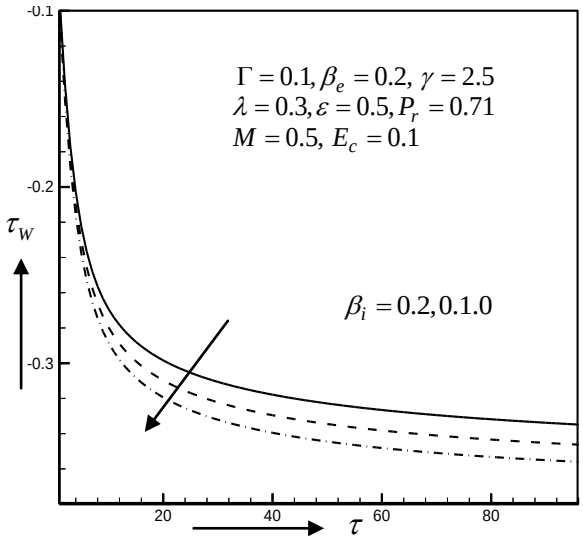

Figure 4(b): Shear stress in z - axis for different values of ion-slip parameter

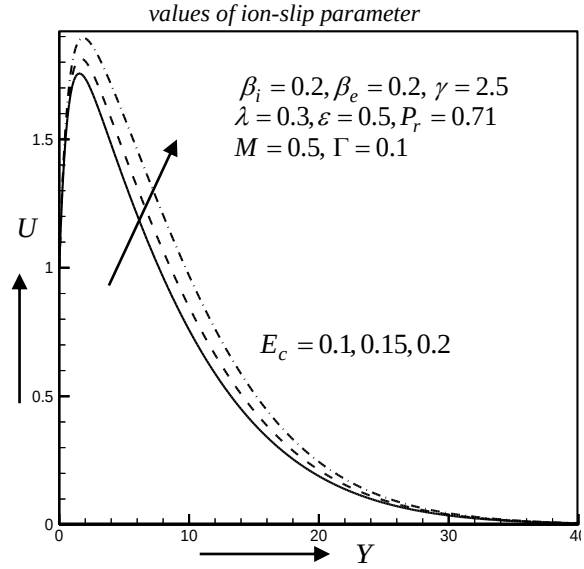

Figure 5(a): Primary velocity profiles for different values of Eckert number

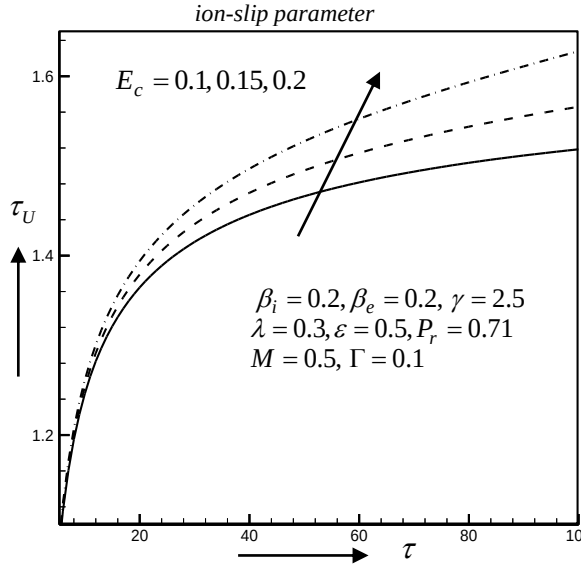

Figure 5(b): Shear stress in x -axis for different values of values of Eckert number

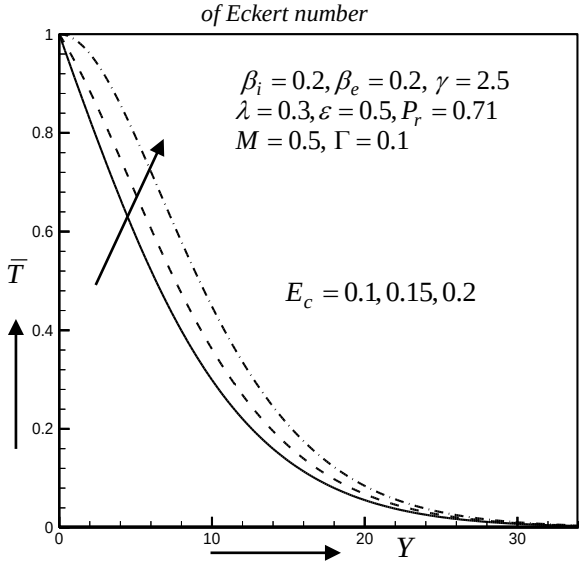

Figure 6(a): Temperature profiles for different values of Eckert number

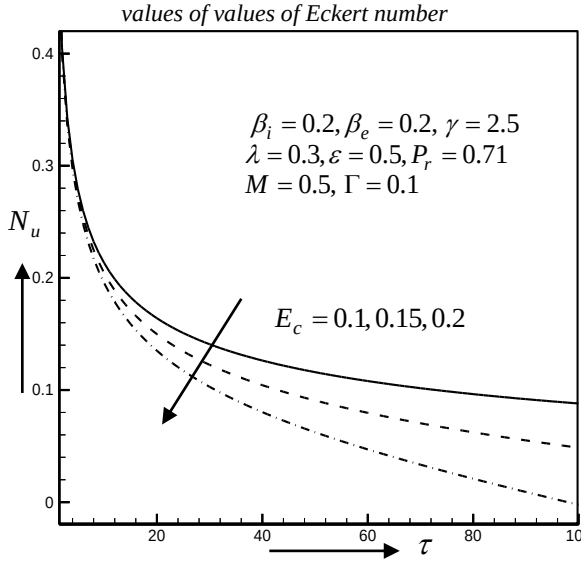

Figure 6(b): Nusselt number profiles for different values of Eckert number

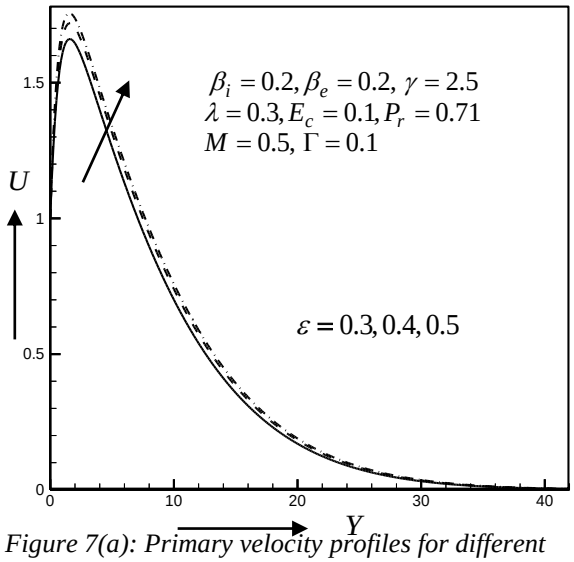

Figure 7(a): Primary velocity profiles for different values of porosity parameter

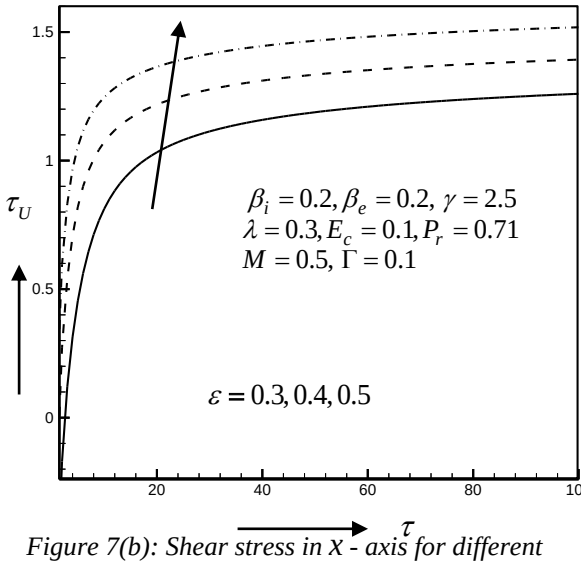

Figure 7(b): Shear stress in x - axis for different values of porosity parameter

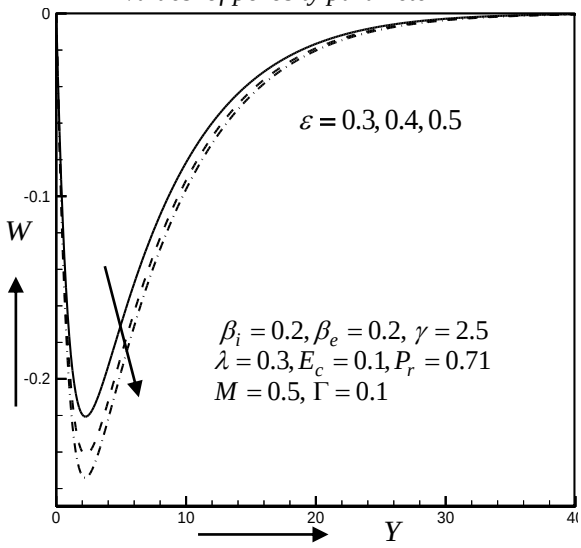

Figure 8(a): Secondary velocity profiles for different values of porosity parameter

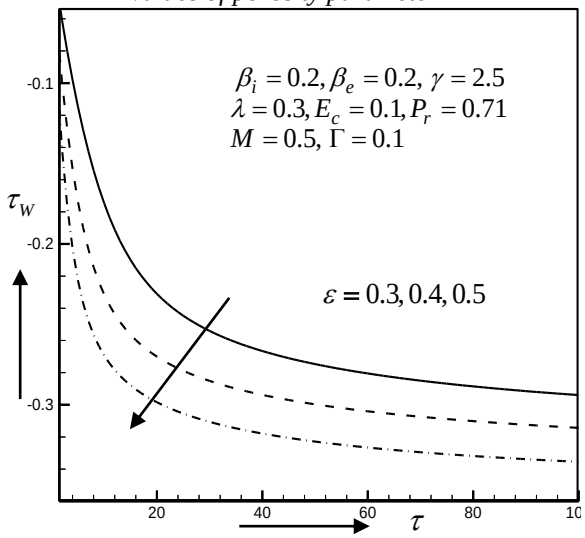

Figure 8(b): Shear stress in z - axis for different values of porosity parameter

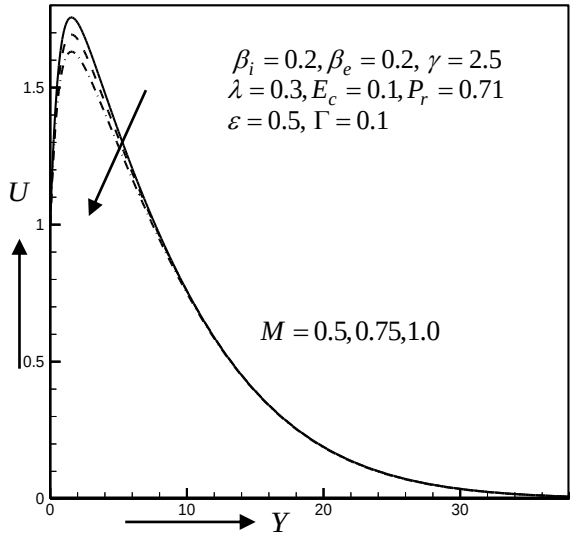

Figure 9(a): Primary velocity profiles for different values of magnetic parameter

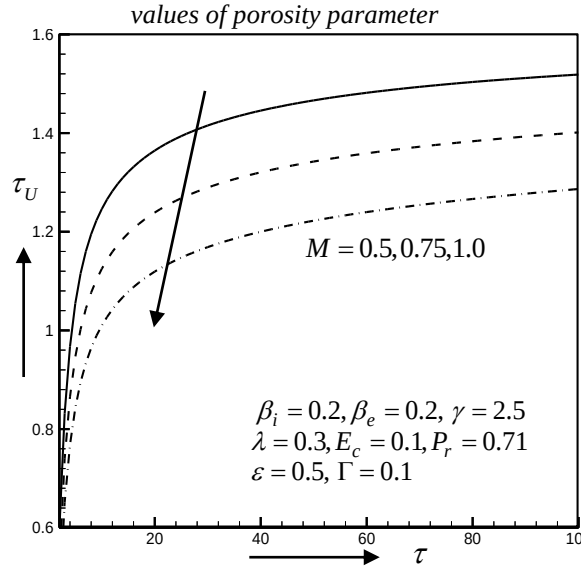

Figure 9(b): Shear stress in x - axis for different values of magnetic parameter

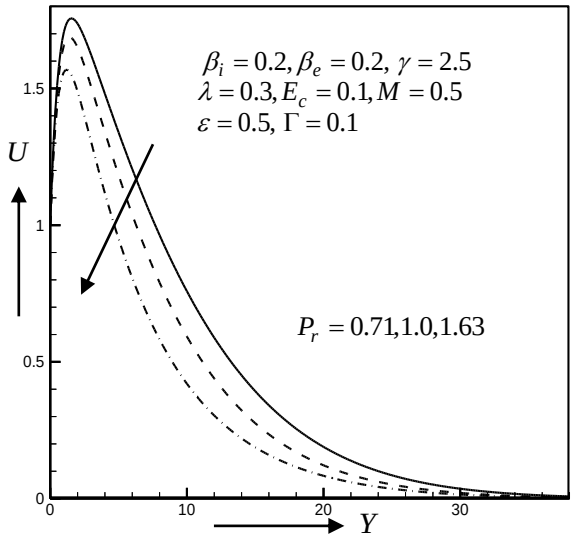

Figure 10(a): Primary velocity profiles for different values of Prandtl number

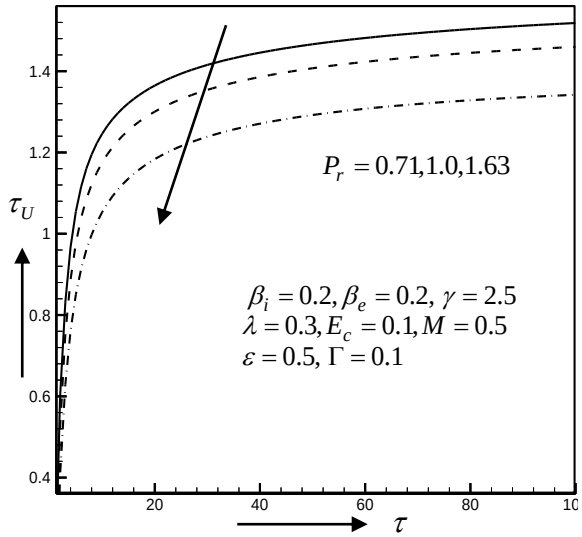

Figure 10(b): Shear stress in X - axis for different values of Prandtl number

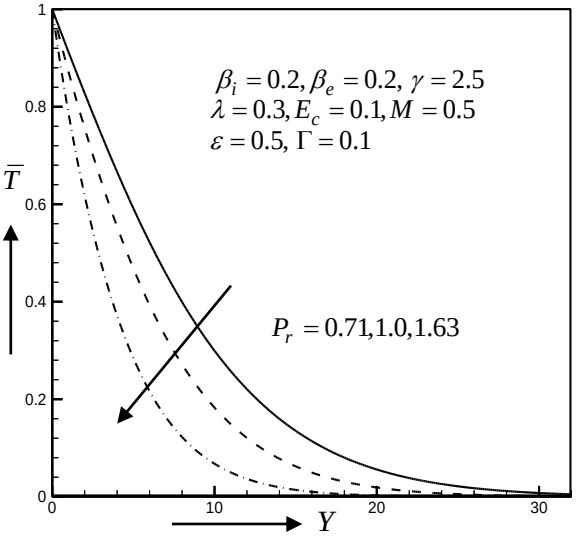

Figure 11(a): Temperature profiles for different values of Prandtl number

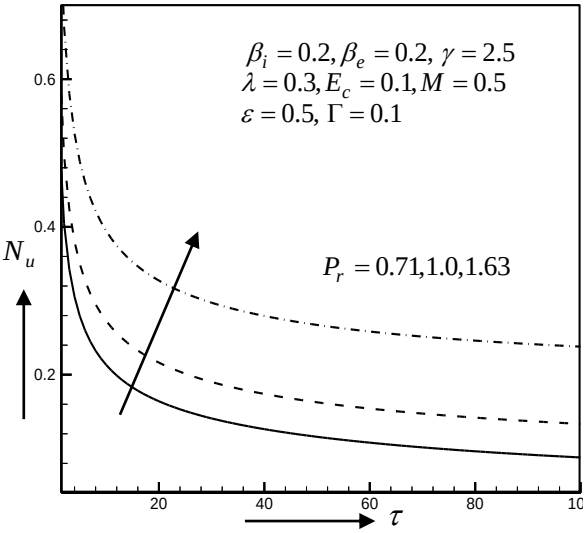

Figure 11(b): Nusselt number profiles for different values of Prandtl number

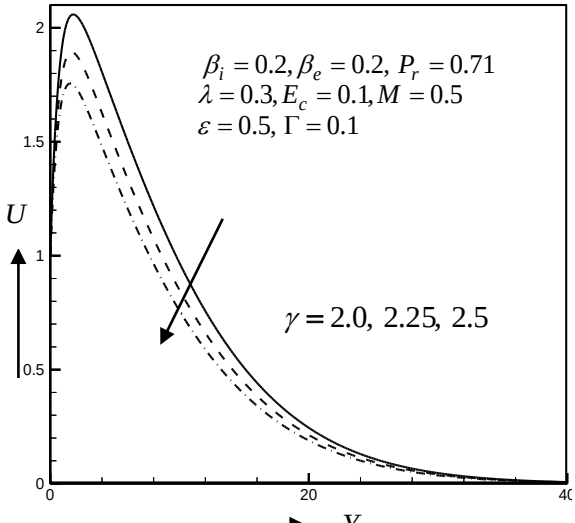

Figure 12(a): Primary velocity profiles for different values of permeability parameter

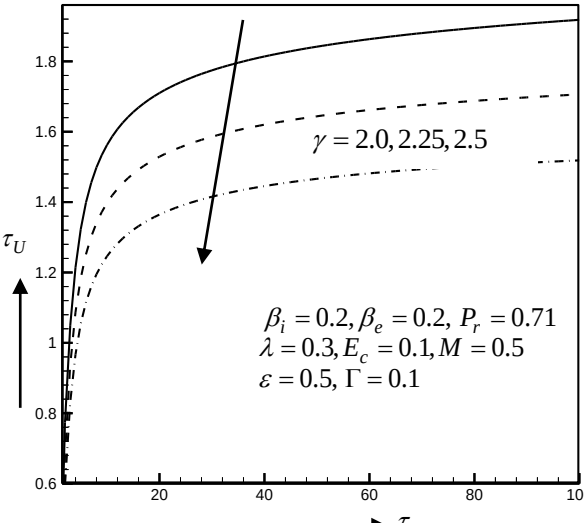

Figure 12(b): Shear stress in x - axis for different values of permeability parameter

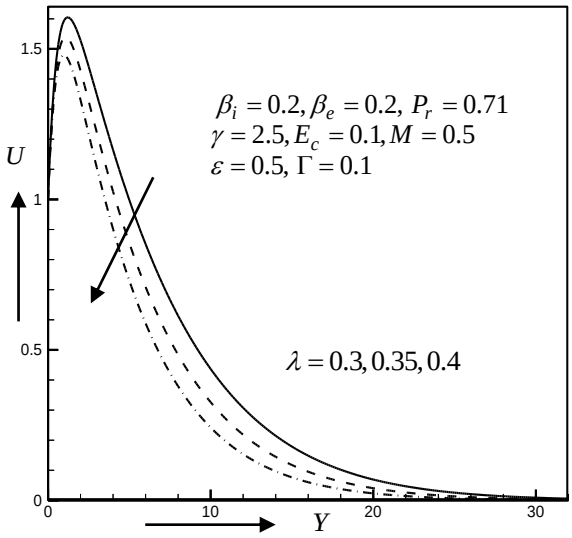

Figure 13(a): Primary velocity profiles for different values of suction parameter

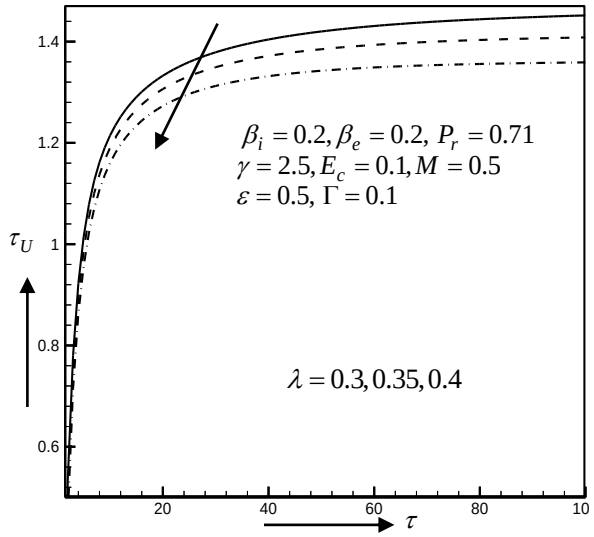

Figure 13(b): Shear stress in x - axis for different values of suction parameter

6. Conclusion

High porosity medium effects on MHD boundary layer unsteady flow with Joule heating and viscous dissipation along a upright porous plate and ion-slip current have been studied numerically. The finite difference method is used to solve the dimensionless coupled nonlinear differential equations. The conclusions of the study are as follows:

a) The primary velocity and shear stress in x-axis increases with increase of ion-slip parameter, Eckert number, porosity parameter whereas these decreases with increases of magnetic parameter, Prandtl number, permeability parameter and suction parameter.

b) The secondary velocity and shear stress in z-axis decreases with increase of ion-slip parameter and porosity parameter.

c) The temperature of the fluid increases with increase of Eckert number while it decreases with increase of Pradtl number.

d) The Nusselt number decreases with increase of Eckert number whereas it increases of Prandtl number.

Acknowledgments

The authors would like to thank to the Ministry of Science and Technology, Government of People's Republic of Bangladesh for providing financial support to enable conducting this research work under the project of Research & Development.

References

[1]. Gebhart B. (1962). Effects of viscous dissipation in natural convection. *Journal of Fluid Mechanics*, 14, 225-235.

[2]. Vafai K. & Tien C.L. (1981). Boundary and inertia effects on flow and heat transfer in porous media, *International Journal of Heat and Mass Transfer*. 24, 195-203. http://dx.doi.org/10.1016/00179310(81)90027-2

[3]. Schwartz C. E. & Smith J. M. (1953). Flow distribution in packed beds. *Industrial & Engineering Chemistry*, 45(6), 1209-1218.

[4]. Dulal Pal, (2010). Magnetohydrodynamic non-Darcy mixed convection heat transfer from a vertical heated plate embedded in a porous medium with variable porosity. *Communication in Nonlinear Science and Numerical Simulation*, 15(12), 3974-3987. http://dx.doi.org/10.1016/j.cnsns.2010.02.003

[5]. Ramachandra Prasad V., Vasu B., AnwarBég O. & Parshad Rana D. (2012). Thermal radiation effects on magnetohydrodynamic free convection heat and mass transfer from a sphere in a variable porosity regime. *Communication in Nonlinear Science and Numerical Simulation*, 17(2), 654-671. http://dx.doi.org/ 10.1016/j.cnsns.2011.04.033.

[6]. Al-Humoud J. M. & Chamkha Ali J. (2006). Double diffusive convection of a rotating fluid over a surface embedded in a thermally stratified high porosity medium. *Head and Technology*, vol. 24(1), 51-59.

[7]. Hemant Poonia, Chaudhary R. C. (2010), MHD free convection and mass transfer flow over an infinite vertical plate with viscous dissipation. *Journal theoretical and applied Mechanics*, 37, No. 4, 263-287. doi:10.2298/TAM1004263P.

[8]. Foisal A. A. & Alam M. M. (2016). Unsteady free convection fluid flow over an inclined plate in the presence of a magnetic field with thermally stratified high porosity medium. *Journal of Applied Fluid Mechanics*, 9, No. 3, 1467-1475. Doi: 10.18869/ acadpub.jafm.68.228.24050.

[9]. Mahender D. & Srikanth Rao P. (2015). Unsteady MHD free convection and mass transfer flow past a porous plate in presence of viscous dissipation. *Journal of Physics: Conference Series* 662(1): 012012, 1-6, doi:10.1088/1742-6596/662/1/012012.

[10]. Jaber Khaled K. (2014), Effects of viscous dissipation and Joule heating on MHD flow of a fluid with variable properties past a stretching vertical plate. *European Scientific Journal*, 10, No.33, 383-393.

[11]. Chamkha Ali J., Takhar Harmindar S. & Guhan Nath, (2005). Natural convection flow in a rotating fluid over a vertical plate embedded in a thermally stratified high porosity medium. *International Journal of fluid Mechanics Research*, 32(5), 511-527. Doi: 10.1615

[12]. Chen C.K., Hung C. I. & Horng H. C. (1987). Transient natural convection on a vertical flat plate embedded in a high porosity medium. *ASME Journal of Energy Resources Technology*, 109(3), 112-118. https://doi.org/10.1115/1.3231335

[13]. Bhuvana Vijaya R. & Mallikarjuna B. (2014). Effect of variable thermal conductivity on convective heat and mass transfer over a vertical plate in a rotating system with variable porosity regime. *Journal of Naval Architecture and Marine Engineering*, 11, 83-92. http://dx. doi. org/ 10.3329

[14]. Anjali Devi S. P., Shailendhra K. & Ramesan C.V. (2012). Hall effect on unsteady MHD free convection flow past an impulsively started porous plate with viscous and Joule's dissipation. *International Journal of Science and Engineering Investigations*, 1, issue 6, 64-71.

[15]. B. Lakshmanna & S. Venkateswarlu (2018), Unsteady MHD convective flow of an incompressible viscous fluid through porous medium over a vertical plate. *Annals of Pure and Applied Mathematics*, 16(2), pp. 451-460. Doi: 10.22457/apam.v16n2a23

[16]. Mohammed Modather Mohammed Abdou, (2017). Effects of MHD and Joule heating on free convective boundary layer with a variable plate temperature in a porous medium. *Applied Mathematical Sciences*, 11(36), 1765 -1777. https://doi.org/10.12988/ams.2017.75168